

Constitutive versus regulated SNARE assembly: a structural basis

Yong Chen¹, Yibin Xu¹, Fan Zhang
and Yeon-Kyun Shin*

Department of Biochemistry, Biophysics and Molecular Biology, Iowa State University, Ames, IA, USA

SNARE complex formation is essential for intracellular membrane fusion. Vesicle-associated (v-) SNARE intertwines with target membrane (t-) SNARE to form a coiled coil that bridges two membranes and facilitates fusion. For the SNARE family involved in neuronal communications, complex formation is tightly regulated by the v-SNARE-membrane interactions. However, it was found using EPR that complex formation is spontaneous for a different SNARE family that is involved in protein trafficking in yeast. Further, reconstituted yeast SNAREs promoted membrane fusion, different from the inhibited fusion for reconstituted neuronal SNAREs. The EPR structural analysis showed that none of the coiled-coil residues of yeast v-SNARE is buried in the hydrophobic layer of the membrane, making the entire coiled-coil motif accessible, again different from the deep insertion of the membrane-proximal region of neuronal v-SNARE into the bilayer. Importantly, yeast membrane fusion is constitutively active, while synaptic membrane fusion is regulated, consistent with the present results for two SNARE families. Thus, the v-SNARE-membrane interaction may be a major molecular determinant for regulated versus constitutive membrane fusion in cells.

The EMBO Journal (2004) 23, 681–689. doi:10.1038/sj.emboj.7600083; Published online 5 February 2004

Subject Categories: structural biology; membranes & transport
Keywords: EPR; membrane fusion; SNARE

Introduction

Fusion of cargo vesicles to the target membrane is the prevailing mechanism for the delivery of fresh lipids and proteins to organelles, and for the secretion of neurotransmitters and hormones. The machinery that brings about intracellular membrane fusion is thought to be built around the SNARE proteins that are widely conserved from yeast to humans (Söllner *et al.*, 1993; Rothman, 1994; Jahn and Südhof, 1999; Lin and Scheller, 2000; Brunger, 2001; Rizo and Südhof, 2002). A crucial step is the formation of the core SNARE complex between the vesicle-associated (v-) SNARE

and the target plasma membrane (t-) SNARE. Conserved coiled-coil motifs from individual SNAREs associate and twist to form a stable helical bundle (Hanson *et al.*, 1997; Lin and Scheller, 1997; Katz *et al.*, 1998; Poirier *et al.*, 1998; Sutton *et al.*, 1998; Antonin *et al.*, 2002, Kweon *et al.*, 2003a).

The SNARE family involved in neurotransmitter release at synapses and that participating in yeast protein trafficking are two best characterized systems (Gerst, 2003; Jahn *et al.*, 2003). In the neuron, an integral membrane protein synaptobrevin is v-SNARE, and syntaxin 1A and SNAP-25 are two t-SNARE proteins residing in the plasma membrane. In yeast, Snc is v-SNARE, while Sso and Sec9 are yeast counterparts of syntaxin and SNAP-25, respectively (Aalto *et al.*, 1993; Protopopov *et al.*, 1993; Brennwald *et al.*, 1994; Ferro-Novick and Jahn, 1994). There are remarkable sequence similarities between these two SNARE families, implying conserved functions (Weimbs *et al.*, 1997).

Perhaps the most profound difference between two fusion systems is the way in which membrane fusion is regulated (Gerst, 2003; Jahn *et al.*, 2003). Yeast fusion machinery is constitutively active to support the steady-state flow of lipids and proteins to cell compartments, although regulatory factors such as Sec1, the N-terminal domain of Sso1p, and protein kinase A have been identified (Nicholson *et al.*, 1998; Jahn and Südhof, 1999; Marash and Gerst, 2001). In contrast, membrane fusion in the neuron is tightly regulated and primarily triggered by the Ca²⁺ signal (Chen *et al.*, 1999). Several regulatory proteins such as Ca²⁺-sensing synaptotagmin (Chapman, 2002; Südhof, 2002), Munc-13 (Augustin *et al.*, 1999; Rosenmund *et al.*, 2002), and complexin (Chen *et al.*, 2002; Pabst *et al.*, 2002) have been found in neuronal cells. At present, the exact roles of individual regulators are not well understood beyond the general belief that SNARE assembly is influenced by the regulators.

Previously, Rothman and co-workers demonstrated that SNAREs are the minimal fusion machinery (Weber *et al.*, 1998). Their results suggest that SNARE complex formation directly promotes membrane fusion. However, it has been recently shown that neuronal v- and t-SNAREs reconstituted into the separate membranes do not spontaneously engage one another to form the complex (Hu *et al.*, 2002; Kweon *et al.*, 2003b). The assistance of other proteins such as calcium sensor appears to be necessary for SNARE assembly and membrane fusion (Hu *et al.*, 2002). The structure of membrane-bound synaptobrevin determined with EPR provided important insights into the mechanism of this regulation of SNARE complex formation (Kweon *et al.*, 2003b). For yeast SNAREs, however, such regulation might not be operative because membrane fusion is constitutively active.

In this work, we demonstrate that yeast v- and t-SNAREs reconstituted on the separate membranes spontaneously associate to form the complex, different from the inhibition observed for neuronal SNAREs (Hu *et al.*, 2002; Kweon *et al.*, 2003b). The EPR results correlated well with the results of fusion that significant membrane fusion was observed for

*Corresponding author. Department of Biochemistry, Biophysics and Molecular Biology, Iowa State University, 4152 Molecular Biology Building, Ames, IA 50011, USA. Tel.: +1 515 294 2530;

Fax: +1 515 294 0453; E-mail: colishin@iastate.edu

¹These authors contributed equally to this work

Received: 13 October 2003; accepted: 2 January 2004; Published online: 5 February 2004

reconstituted yeast SNAREs in the fusion assay, while no fusion was detected for reconstituted neuronal SNAREs under biologically relevant conditions. Further, using EPR, we examined the structure and the membrane topology of reconstituted yeast v-SNARE Snc2p. It was found that none of the amino acids in the coiled-coil motif is deeply inserted into the acyl chain region of the bilayer, making the coiled-coil motif fully available for complex formation.

Results

EPR assay of core SNARE complex formation

The coiled-coil motif of yeast v-SNARE Snc is largely unstructured and freely moving in solution. However, when complexed with t-SNAREs (Couve and Gerst, 1994; Rossi *et al*, 1997), the polypeptide becomes α -helical (Nicholson *et al*, 1998), which significantly reduces the degree of freedom for the peptide backbone as well as for the amino-acid side chains. Site-directed spin labeling (SDSL) and EPR spectroscopy are very effective in detecting such secondary structural changes (Hubbell *et al*, 1998, 2000).

In SDSL, native amino acids are site-specifically replaced one by one with cysteines, to which the nitroxide side chain is attached. The EPR line shape is sensitive to the motional rates of the nitroxide. The helix formation usually involves a large EPR line-shape change from a narrow spectrum reflecting the fast motion of the nitroxide to a broad spectrum reflecting the slow motion (Hubbell *et al*, 1996; Mchaourab *et al*, 1996). Further, with SDSL, conformational changes can be monitored at various locations of the polypeptide chain.

First, as a control, we examined the core complex formation between soluble SNAREs using SDSL and EPR spectroscopy. Soluble parts of individual SNAREs containing coiled-coil motifs Sso1pH3 (amino acids 185–265 of Sso1p), Sec9c (amino acids 401–651 of Sec9), and Snc2pS (amino acids 1–93 of Snc2p) were subcloned and expressed in *Escherichia coli*. The purity of all recombinant proteins was examined by the SDS-PAGE analysis after purification (Figure 1A). For EPR measurements, five spin-labeled mutants of Snc2pS covering the coiled-coil motif (R32C, I46C, G53C, E60C, and G76C) were prepared and labeled with methanethiosulfonate spin label (MTSSL). EPR spectra of spin-labeled Snc2pS were all narrow, reflecting the fast motion of the nitroxide, characteristic of a freely moving random coil (Figure 2B). However, as expected, the addition of

t-SNAREs Sec9c and Sso1pH3 changed the EPR spectra to all broad, reflecting the slow motion of the nitroxides, which indicates the transition from an unstructured state to the helical structure due to spontaneous core complex formation (Figure 2C).

Next, recombinant SNAREs containing transmembrane domains (TMD) Sso1pHT (amino acids 185–290 of Sso1p)

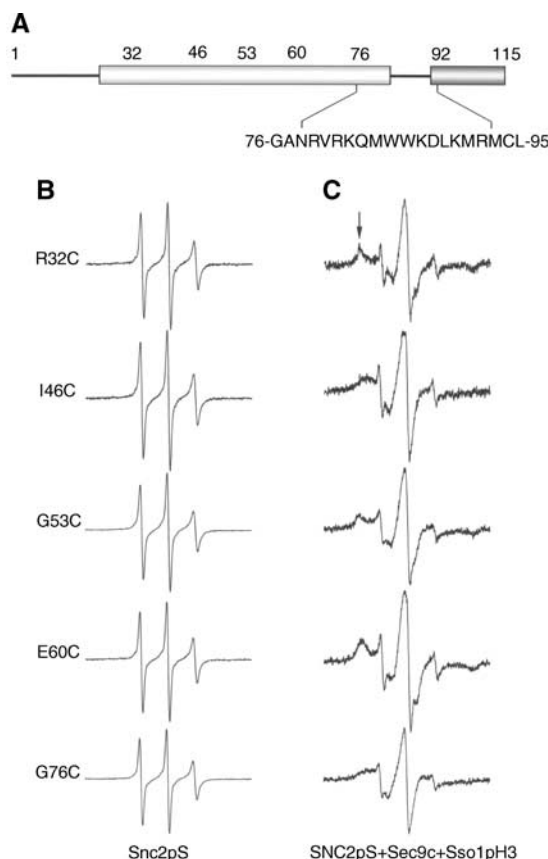


Figure 2 SDSL EPR detects SNARE complex formation at various positions. (A) Spin-labeled positions are indicated on the primary structural diagram. Amino-acid sequence from positions 76–95 is shown. (B) Room temperature EPR spectra for spin-labeled Snc2pS at various positions. (C) Spectra for Snc2pS after mixing with the four-fold molar excess of Sec9c and Sso1pH3. The arrows indicate the immobile spectral component resulting from the formation of SNARE complexes.

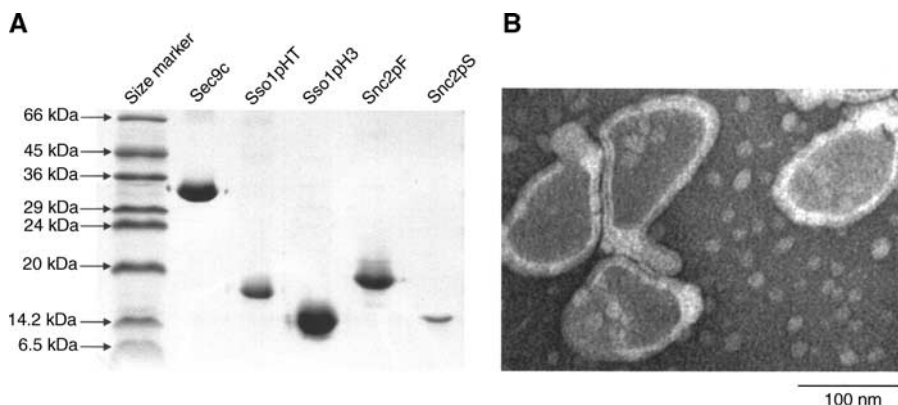


Figure 1 Characterization of SNARE samples. (A) SDS-PAGE analysis of recombinant SNARE proteins used in this study. (B) Electron micrograph of negatively stained Snc2pF-reconstituted vesicles.

and Snc2pF (amino acids 1–115 of Snc2p) were examined with EPR. Five cysteine mutants of Snc2pF at the same positions (R32C, I46C, G53C, E60C, and G76C) were prepared for spin labeling (Figure 2A). Again, the purity of SNARE proteins was examined with SDS–PAGE (Figure 1A). Spin-labeled mutants were then reconstituted into 1-palmitoyl-2-oleoylphosphatidylcholine (POPC) vesicles containing 15 mol% negatively charged dioleoylphosphatidylserine (DOPS), a lipid composition commonly used to mimic the native cellular membrane (Weber *et al*, 1998; Parlati *et al*, 1999; McNew *et al*, 2000). We reconstituted t-SNAREs into separate vesicles of the same lipid composition for the mixing experiment. After reconstitution, the integrity of vesicles was verified with negative-staining electron microscopy (Figure 1B). Except for G76C, EPR spectra are narrow and reflect the fast motion of the nitroxide, indicating that the coiled-coil motif region is largely unstructured and freely moving (Figure 3A). The spectrum for membrane-proximal G76C is relatively broad, most likely due to the membrane–peptide interaction because the polypeptide chain is anchored to the membrane via TMD (see below). However, when mixed with soluble t-SNAREs or vesicles carrying t-SNAREs,

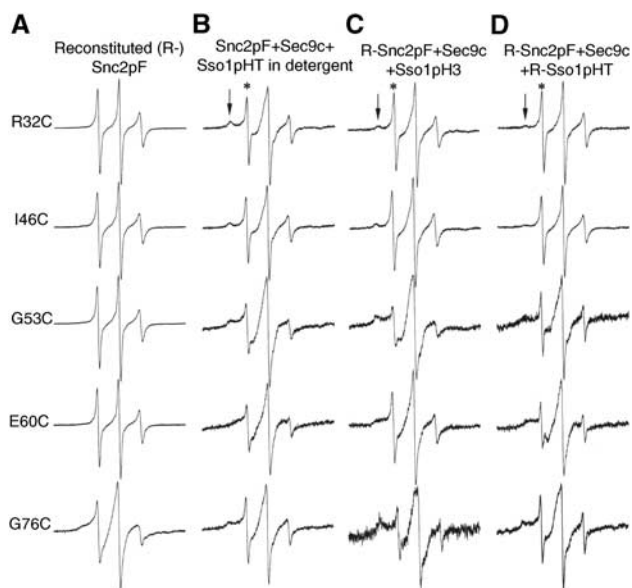


Figure 3 EPR assay of SNARE complex formation. (A) EPR spectra for reconstituted (R-) Snc2pF mutants. (B) EPR spectra for detergent solubilized Snc2pF mutants after mixing with Sso1pHT and Sec9c. EPR spectra are composed of two components: the sharp one (*) representing uncomplexed Snc2pF and the broad one (arrows) representing the SNARE complex. For each spin-labeled mutant, the composite spectrum is basically the sum of the spectrum in (A) and the spectrum similar to those in Figure 2C, in an appropriate ratio. The standard spectral decomposition analysis (Thorgeirsson *et al*, 1996) provides the fraction of Snc2pF in the complex (f_{complex}) and that in an unstructured form (f_{free}). For each mutant, the percentage of complex formation was calculated from the equation $[f_{\text{complex}}/(f_{\text{complex}} + f_{\text{free}}) \times 100]$: R32C, 68%; I46C, 60%; G53C, 84%; E60C, 82%; and G76C, 40%. (C) EPR spectra for R-Snc2pF mixed with Sso1pH3 and Sec9c (soluble t-SNAREs) in the absence of the detergent. The percentages of complex formation for individual mutants are: R32C, 60%; I46C, 62%; G53C, 91%; E60C, 76%; and G76C, 50%. (D) EPR spectra taken after mixing R-Snc2pF with R-Sso1pHT and Sec9c. The percentages of complex formation for individual mutants are: R32C, 38%; I46C, 33%; G53C, 82%; E60C, 85%; and G76C, 49%. In all cases, the four-fold molar excess of t-SNAREs was mixed with reconstituted v-SNARE mutants.

we observed the broad component (arrows in Figure 3C and D) for all mutants, clearly indicating that SNARE complex formation has occurred, consistent with the previous reported results (McNew *et al*, 2000). EPR spectra were collected at 20°C within 30 min after mixing t- and v-SNAREs. There were no significant further spectral changes after 30 min.

For reconstituted SNAREs, complex formation is less than quantitative. The narrow spectral components (asterisks in Figure 3) represent unstructured Snc2pF that does not participate in complex formation. The standard spectral decomposition analysis (see the legend of Figure 3) revealed that the percentages of complex formation for Snc2pF range from 33 to 91%, depending on the spin-labeled positions, indicating some but not serious perturbations due to spin labeling.

Such spontaneous SNARE assembly for the yeast system is quite different from what has been observed for neuronal SNAREs for which SNARE complex formation is inhibited due to the v-SNARE–membrane interactions (Kweon *et al*, 2003b). EPR is sufficiently sensitive to detect small spectral changes due to complex formation, as little as a few percents. No spectral changes were detected for reconstituted neuronal SNAREs within experimental uncertainty (Kweon *et al*, 2003b; see the Supplementary data), indicating negligible SNARE complex formation.

Membrane-bound structure of Snc2pF

To explore the structural basis for spontaneous complex formation for reconstituted yeast SNAREs, we investigated the membrane-bound structure of Snc2pF using SDSL EPR. For neuronal SNARE assembly, it was found that the COOH-terminal end of the v-SNARE coiled-coil motif plays a key role in inhibiting neuronal SNARE assembly. This region inserts deeply into the membrane with high affinity, reducing its accessibility to t-SNAREs, which perhaps restricts SNARE assembly kinetically and thermodynamically (Kweon *et al*, 2003b).

We prepared 20 consecutive spin-labeled mutants of Snc2pF (G76C–L95C) for SDSL EPR. After reconstitution into the membrane, the EPR spectra of spin-labeled mutants were collected at room temperature (Figure 4). From G76C through R81C, EPR spectra are composed of two components. The narrow component represents the freely moving polypeptide chain in the solution phase. The broad component represents the species interacting with the membrane surface. However, from K82C through L95, EPR spectra display mainly broad lineshapes, typical for the nitroxides interacting fully with the viscous bilayer (Rabenstein and Shin, 1995). We do not observe any sign of the spin–spin coupling in the EPR spectra, suggesting that synaptobrevin is mostly monomeric.

The EPR saturation method to measure accessibilities (Altenbach *et al*, 1994) was used to characterize the secondary structure and membrane topology of yeast v-SNARE Snc2pF at the water–membrane interface (Kim *et al*, 2002; Kweon *et al*, 2002). We measured the accessibility of the nitroxide to a water-soluble paramagnetic reagent, nickel-ethylenediaminediacetic acid (NiEDDA) (W_{NiEDDA}), to estimate the solvent exposure of the spin-labeled site. We also determined the accessibility to a nonpolar paramagnetic reagent, molecular oxygen (W_{O_2}), to probe the immersion into the membrane interior.

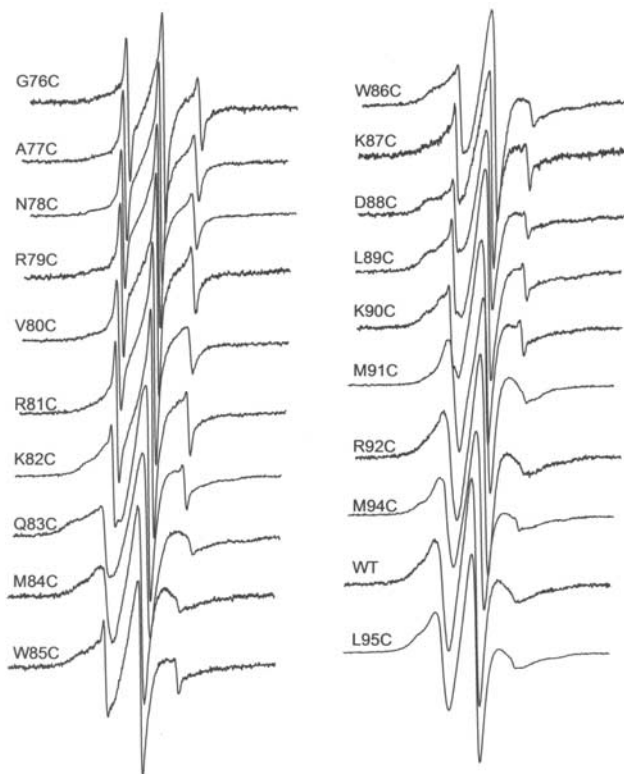


Figure 4 Room temperature EPR spectra for the interfacial region of reconstituted (R-) Snc2pF. We note that the EPR spectrum for G76C here is slightly different from that in Figure 3A: the sharp component is a little less in the latter. The spectral decomposition analysis of the spectrum of G76C in Figure 4 indicated that there was an approximately 5% contamination of freely diffusing free spin species in the sample, which should not alter the accessibility parameter values. The first derivative mode presentation of EPR spectra makes such small contamination conspicuous.

For reconstituted Snc2pF, an overall decrease in W_{NiEDDA} was observed along the sequence, while an overall increase was detected for W_{O_2} (Figure 5A). Importantly, we notice substantial peaks and valleys in the region of 84–91, suggesting the presence of a secondary structure. It was previously found that the ratio of W_{O_2} to W_{NiEDDA} is proportional to the immersion depth of spin label. The immersion depths were calculated from the standard curve (Altenbach *et al*, 1994; Macosko *et al*, 1997).

The immersion depths show a periodic oscillation in the region of residues 84–91. We fit the data with a sine function with an additional variable that incorporates the tilt of the helix with respect to the membrane. The immersion depth results fit well with an α -helical geometry in this region (Figure 5B). In addition, the fitting suggested that this short two-turn helical segment has a tilted orientation, at an angle of 40° with respect to the membrane normal (Macosko *et al*, 1997; Kweon *et al*, 2003b).

We note that EPR reported an immersion depth of $\sim 11 \text{ \AA}$ for position 90, for which the native residue is lysine. However, it is likely that the location of the lysine side chain is shallower. The positive charge on K90 could snorkel out to seek the negative charges on phosphate, in contrast to what is expected for a relatively nonpolar nitroxide side chain.

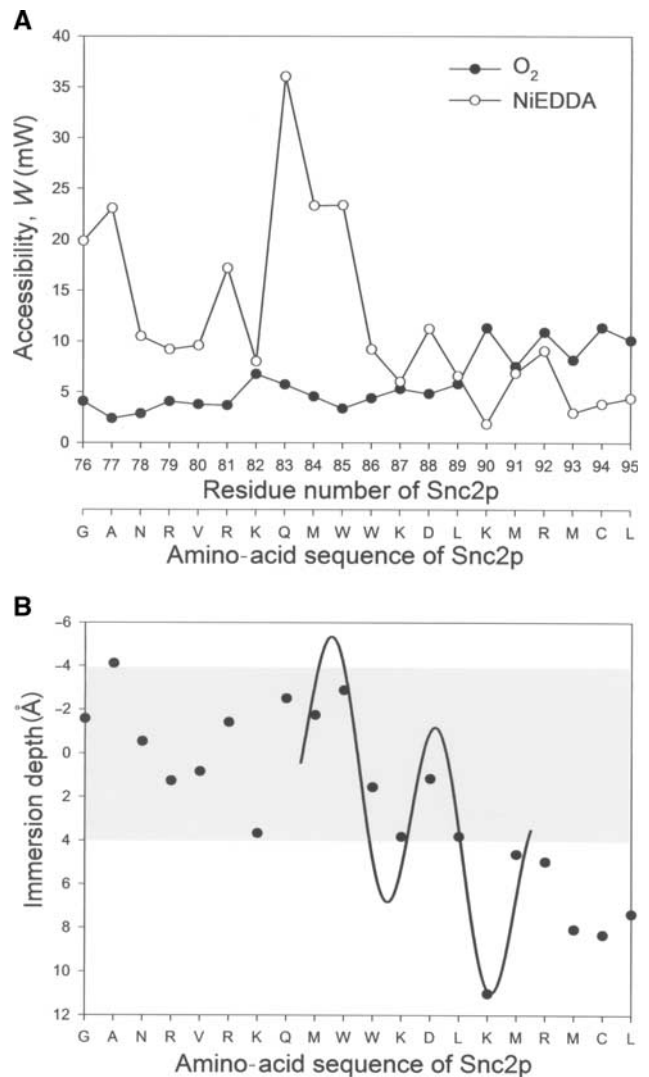


Figure 5 EPR accessibility measurements. (A) Accessibility parameters W_{O_2} (closed circles) and W_{NiEDDA} (open circles) are plotted against the amino-acid sequence. (B) Membrane immersion depths versus the amino-acid sequence of Snc2pF. The head group region of the lipid vesicles is shown shaded. The solid line represents the fit on the basis of a tilted α -helical model (see text). Typical accessibility parameter values for the fully exposed residues are approximately 30 and 4 mW for NiEDDA and O_2 , respectively, and typical W_{NiEDDA} and W_{O_2} values for the fully membrane-inserted residues are around 2 and 12 mW, respectively.

Comparison of membrane topologies of yeast Snc2pF and neuronal synaptobrevin

It appears that yeast Snc2pF and neuronal synaptobrevin share similar overall membrane topology: The long unstructured region is connected to the short helical segment that enters the membrane with an oblique angle. Presumably, the short helical segment is joined to the membrane-spanning α -helical TMD via a few disordered residues (Figure 6) (Kweon *et al*, 2003b).

However, the difference between two structures does exist with the location of the short helical segment along the primary sequence. For synaptobrevin, the helical segment is part of the coiled-coil motif, and it is oriented in such a way that the membrane-seeking tryptophan (Trp) residues are located near the C-terminal end of the segment. As a result,

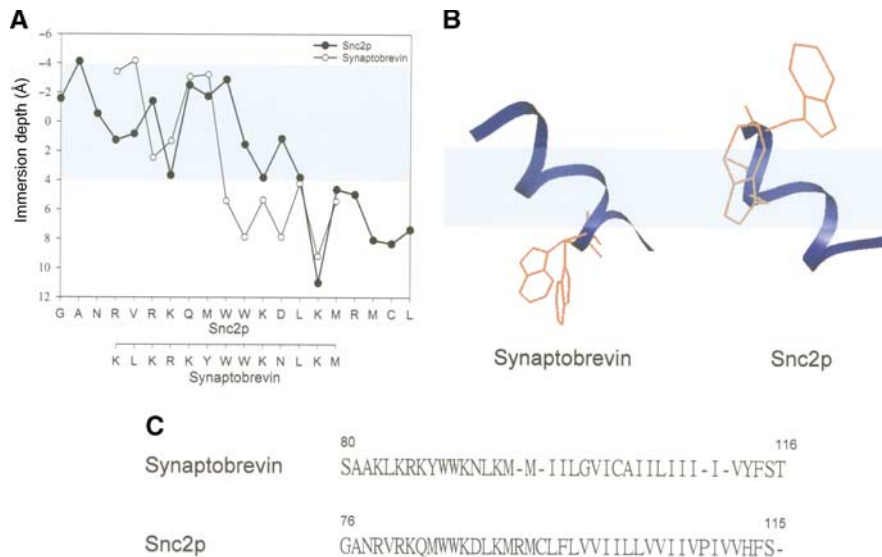


Figure 6 Comparison of membrane topologies of the interfacial regions between neuronal and yeast v-SNAREs. **(A)** Membrane immersion depths of Snc2pF (closed circles) and those of synaptobrevin (open circles). The shaded region is the head group of the lipid bilayer. **(B)** Topological models for Snc2p and synaptobrevin. Amino-acid side chains for two interfacial tryptophans are shown highlighted. **(C)** Sequence alignment of the membrane-proximal regions of synaptobrevin and Snc2p.

two Trp residues are inserted deep into the acyl chain region of the bilayer (Yau *et al*, 1998; Kweon *et al*, 2003a). In contrast, for Snc2pF, two Trp residues are located near the beginning of the short helical segment. Moreover, the orientation of the helix makes two Trp residues point upward and makes deep penetration into the membrane difficult (Figure 6B). Consequently, the affinity of the short helical segment to the membrane for Snc2p is likely to be much lower than that for neuronal synaptobrevin (Thorpeirsson *et al*, 1996; Wimley and White, 1996).

Further, the crystal structure of the neuronal core SNARE complex suggests that the coiled coil terminates at residue 92 for synaptobrevin (Sutton *et al*, 1998). On the basis of the sequence alignment, the corresponding terminal residue for Snc2pF should be position 89 (Figure 6C). If this is true, none of the amino acids in the coiled-coil motif appears to be inserted into the acyl chain region of the bilayer for Snc2pF (Figure 5A), suggesting some but weak affinity of the interfacial region to the membrane.

One might argue that the substitution of the nitroxide side chain might have contributed somewhat to the discrepancy between neuronal and yeast v-SNAREs. We compared the fluorescence quenching of Trp residues by lipid quenchers in which fluorescence-quenching bromines are attached to the acyl chain (Figure 7) (Chattopadhyay and London, 1987; Abrams and London, 1992). It is shown that added lipid quenchers (6,7)- and (11,12)-PC influence the Trp fluorescence of Snc2pF much less than it does for synaptobrevin, which suggests that Trp residues of synaptobrevin are deeper in the membrane than those of Snc2p, consistent with the EPR results.

Proteoliposome fusion assays support the structure-based regulatory mechanism

SNARE assembly might drive membrane fusion. Since reconstituted yeast SNAREs form the complex spontaneously, in

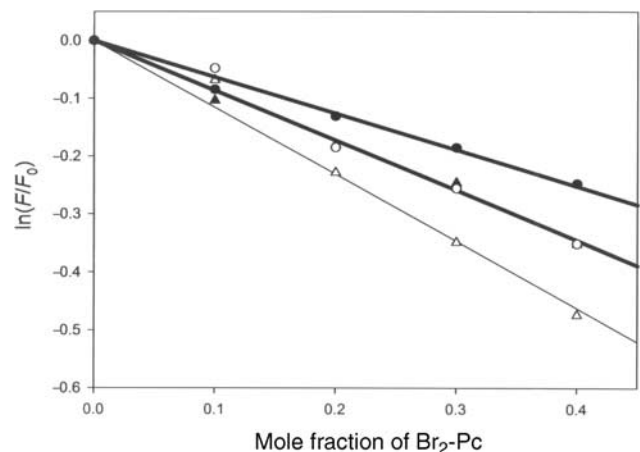


Figure 7 Comparison of fluorescence quenching by lipid quenchers for the two Trp residues between Snc2pF and synaptobrevin. The logarithm of the ratio $\ln(F/F_0)$, where F_0 is the fluorescence intensity in the absence and F is that in the presence of the lipid quencher, is plotted against the mole fraction of 6,7-Br₂-PC for synaptobrevin (open triangles) and Snc2pF (closed triangles), and the mole fraction of 11,12-Br₂-PC for synaptobrevin (open circles) and Snc2pF (closed circles).

contrast to the inhibition of neuronal SNARE assembly, we expect spontaneous membrane fusion with yeast SNAREs. To test this, we reconstituted Sso1pHT into POPC vesicles containing 15 mol% DOPS. We also reconstituted Snc2pF into the separate vesicles of the same lipid composition, but with fluorescent lipids for the measurement of lipid mixing. In both cases, the lipid-to-protein ratio was approximately 300:1.

First, as a control, we mixed Sso1pHT-reconstituted vesicles and Snc2pF-reconstituted vesicles without Sec9c. Over a period of 100 min, we did not observe any fluorescence

change (black line in Figure 8). However, when we preincubated Sso1pHT-reconstituted vesicles with sec9c for 30 min and subsequently mixed this solution with Snc2pF-reconstituted vesicles, we observed the slow but steady increase of fluorescence signal (red line in Figure 8), indicating lipid mixing. The fluorescence change detected in the period of 6000 s corresponds to one 'round of fusion' on the basis of the calculation given by Rothman and coworkers (McNew *et al*, 2000).

In sharp contrast, when neuronal SNAREs were tested under identical conditions, we did not observe any fluorescence change (blue line in Figure 8), indicating that no lipid mixing had occurred during the period of nearly 2 h. The results are in accordance with the previous EPR data that suggest the inhibition of neuronal SNARE assembly under such conditions. However, our current results are quite different from those from the Rothman fusion assay in which slow but apparent lipid mixing was observed (Weber *et al*, 1998). The Rothman fusion assay required an unnatural lipid-to-protein ratio of ~20:1 for vesicular SNARE synaptobrevin, which is exceedingly higher than the ratio of 150–1000:1 in natural synaptic vesicles (Weber *et al*, 1998; Kweon *et al*, 2003b). Thus, the results from the lipid-mixing fusion assays are fully consistent with the present EPR data, and

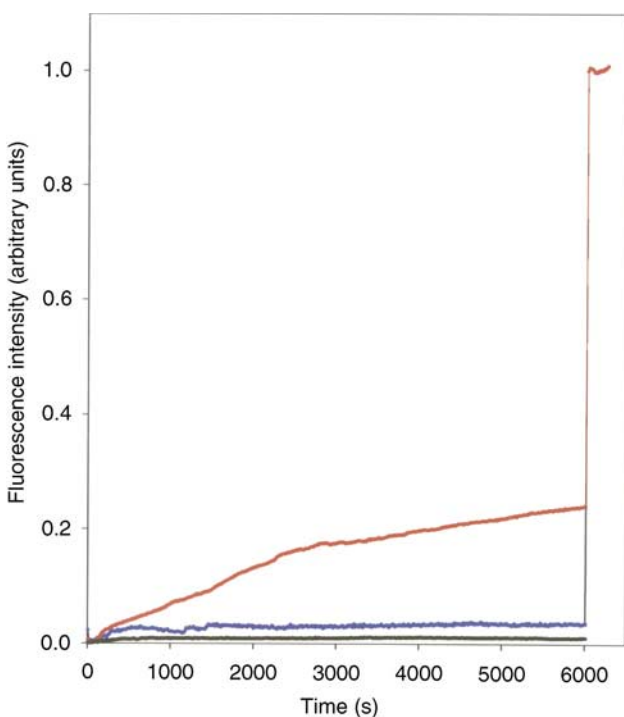


Figure 8 Lipid-mixing fusion assays monitored by fluorescence. The donor/acceptor pairs N-Rh-PE/N-NBD-PE were incorporated into the vesicles containing v-SNARE. Fusion between v-SNARE-reconstituted vesicles and t-SNARE-reconstituted vesicles leads to the dilution of dyes and, consequently, an increase in the average distance between the donor and the acceptor, which results in an increase in donor fluorescence. The red line is the time trace of the fluorescence change after mixing reconstituted yeast v- and t-SNAREs. The black line is the control run after mixing only reconstituted Sso1pHT and reconstituted Snc2pF without adding Sec9c. The blue line is the time trace for neuronal SNAREs, indicating virtually no lipid mixing. The fusion reaction was terminated by introducing 1% (v/v) Triton X-100, which results in the sudden jump in the fluorescence intensity.

support the proposed mechanism for the regulation of SNARE assembly and membrane fusion by the membrane.

The time scale of membrane fusion appears to be much slower than the time scale of SNARE assembly assayed by EPR. We, however, note that the protein concentration used in the fusion assay is at least 10 times less than that used for the EPR assay, which is qualitatively in line with the difference between the two time scales, warranting further investigation.

Discussion

Yeast v-SNARE Snc2p shares 50% sequence identity with the neuronal counterpart synaptobrevin (Figure 6C). Further, the EPR results suggest that the structure and the membrane topology of Snc2p are generally similar to those of synaptobrevin. Yet, there are significant differences between the two in the detailed arrangement of amino acids in the topological structure. For neuronal synaptobrevin, the COOH-terminal region of the coiled-coil motif is deeply inserted into the membrane, restricting the accessibility of the region for SNARE assembly. Particularly, two Trp residues, which are anchored in the acyl chain region of the bilayer, help stabilize the short helical segment in the membrane. This membrane-embedded segment controls the fate of the entire coiled-coil motif for complex formation (Kweon *et al*, 2003b). In contrast, the interfacial residues of Snc2p are bound shallow in the polar surface of membrane and none of the coiled-coil residues is anchored into the acyl chain region of the bilayer. This is likely to make the whole coiled-coil motif accessible to t-SNAREs for complex formation.

There are several factors that might have contributed to the topological differences between the two systems. First, the putative TMD of synaptobrevin is three residues shorter than that of Snc2p (Figure 6C). Therefore, the interfacial region of synaptobrevin could be pulled more towards the membrane than it is for Snc2p. Second, for Snc2p, position 88 is negatively charged aspartic acid, whereas the corresponding residue in synaptobrevin is asparagine. In an attempt to understand the effect of the aspartic acid to asparagine mutation, we made the D88N mutant of Snc2p. However, this mutation alone did not alter the ability of Snc2p to interact with t-SNAREs spontaneously. Therefore, it appears that multiple factors contribute cooperatively to the better stability of synaptobrevin in the membrane than Snc2p.

In conclusion, using EPR assay, we have demonstrated that yeast SNARE assembly is spontaneous (Figure 3), leading to spontaneous membrane fusion (red line in Figure 8). In contrast, neuronal SNARE assembly is tightly regulated (Kweon *et al*, 2003b), resulting in the inhibition of membrane fusion (blue line in Figure 8). Interestingly though, the EPR results suggested that yeast Snc2p shares the same global membrane topology with neuronal synaptobrevin. However, unlike the case with synaptobrevin, the coiled-coil motif of Snc2p floats in or above the polar region of the bilayer, so that it may readily engage with t-SNAREs to form the SNARE complex. The yeast-trafficking fusion machinery is constitutively active and need not be regulated, in sharp contrast to the tightly regulated neuronal exocytosis. Further, the key neuronal regulatory proteins such as synaptotagmin are not found in yeast systems. Therefore, although speculative, the EPR data might suggest that the v-SNARE–

membrane interaction plays a central role in determining whether particular membrane fusion machinery should be regulated or constitutive.

Materials and methods

Plasmid constructs and site-directed mutagenesis

Genes for yeast SNAREs were obtained from Dr James McNew at Rice University. DNA sequences encoding Sso1pH3 (amino acids 185–265), Sso1pHT (amino acids 185–290), Snc2pS (amino acids 1–93), and Snc2pF (amino acids 1–115) are inserted into the pGEX-KG vector between *EcoRI* and *HindIII* sites as N-terminal glutathione

S-transferase (GST) fusion proteins. Sec9c (amino acids 401–651) is inserted into pET-24b(+) between *NdeI* and *XhoI* sites as a C-terminal His₆-tagged protein. In order to introduce a unique cysteine residue for the specific nitroxide attachment, native cysteine 266 of Sso1pHT and native cysteine 94 of Snc2pF were mutated to alanines. QuickChange site-directed mutagenesis (Stratagene) was used to generate all mutants and DNA sequences were confirmed by the Iowa State University DNA Sequencing Facility.

Protein expression, purification, and spin labeling

Recombinant GST fusion proteins were expressed in *E. coli* Rosetta (DE3) pLysS (Novagene). The cells were grown at 37°C in LB medium with glucose (2 g/l), ampicillin (100 µg/ml), and chloramphenicol (25 µg/ml) until the *A*₆₀₀ reached 0.6–0.8. Isopropyl-β-D-thiogalactopyranoside (IPTG) was added to a final concentration of 1 mM. The cells were grown further for four more hours at 22°C. The cell pellets were collected by centrifugation at 6000 r.p.m. for 10 min.

GST fusion proteins were purified by affinity chromatography using glutathione-agarose beads (Sigma). The frozen cell pellet was resuspended in resuspension buffer (phosphate-buffered saline, pH 7.4, with 0.5% Triton X-100 (v/v), PBST) with 2 mM 4-(2-aminoethyl)benzenesulfonyl fluoride (AEBSF) and 5 mM dithiothreitol (DTT). The cells were broken by sonication on an ice bath. For Snc2pF and Sso1pHT, 1% of *n*-lauroyl sarcosine was added to the solution before sonication. The cell lysate was centrifuged at 15000 × *g* for 20 min at 4°C. The supernatant was mixed with glutathione-agarose beads in the resuspension buffer and nutated at 4°C for 40 min. The protein-bound beads were washed with an excess volume of washing buffer (phosphate-buffered saline, pH 7.4). For Sso1pHT and Snc2pF, 0.2% (v/v) Triton X-100 was added, while no detergent was added for Sso1pH3 and Snc2pS when washing. The beads were then washed with thrombin cleavage buffer (50 mM Tris-HCl, 150 mM NaCl, 2.5 mM CaCl₂, pH 8.0), either with 0.2% Triton X-100 for Sso1pHT and Snc2pF, or without detergent for Sso1pH3 and Snc2pS. Finally, the proteins were cleaved from the resin by thrombin (Sigma) at room temperature for 40 min. AEBSF was added to the protein after cleaving from the resin (2 mM final concentration). The protein was stored at –80°C with 10% glycerol.

Cysteine mutants of Snc2pF were spin-labeled before thrombin cleavage. After the cell lysate was incubated with beads and washed with PBS buffer with 0.2% Triton X-100, DTT was added to a final concentration of 5 mM at 4°C for 40 min. The beads were then washed eight times with an excess volume of PBS buffer with 0.2% Triton X-100 to remove DTT. An approximately 20-fold excess of (1-oxyl-2,2,5,5-tetramethylpyrrolinyl-3-methyl)methanethiosulfonate spin label (MTSSL) was added to the protein, and the reaction mixture was left overnight at 4°C. Free MTSSL was removed by washing with excess PBS buffer with 0.2% Triton X-100. The proteins were cleaved by thrombin in cleavage buffer with 0.2% Triton X-100.

The His₆-tagged protein Sec9c was expressed in *E. coli* Rosetta (DE3) pLysS. The cells were grown at 37°C in LB medium with glucose (2 g/l), kanamycin (30 µg/ml), and chloramphenicol (25 µg/ml) until the *A*₆₀₀ reached 0.6–0.8. After the addition of IPTG (1 mM), the cells were grown further for four more hours at 30°C. The cell pellets were collected by centrifugation at 6000 r.p.m. for 10 min.

For purification, the frozen cell pellet was resuspended in lysis buffer (PBS buffer with 20 mM imidazole, 0.5% Triton X-100, 2 mM

AEBSF, pH 8.0). After sonication on ice, the cell lysate was centrifuged at 15000 *g* for 15 min at 4°C. The supernatant was mixed with nickel-nitrilotriacetic acid-agarose beads (Qiagen) in lysis buffer. The mixture was nutated for binding at 4°C for 40 min. After binding, the beads were washed with washing buffer (PBS buffer with 50 mM imidazole, pH 8.0). Then the protein was eluted by elution buffer (PBS buffer with 250 mM imidazole, pH 8.0). The protein can be kept at –80°C with 10% glycerol. All purified proteins were examined with 15% SDS-PAGE.

Membrane reconstitution and electron microscopy

Large unilamellar vesicles (~100 nm in diameter) of POPC containing 15 mol% of DOPS were prepared in cleavage buffer containing no detergent using an extruder. The total lipid concentration was 100 mM. Proteins were mixed with vesicles at an ~1:300 protein-to-lipid molar ratio. The detergent was removed by treating the sample with Bio-beads SM2 (Bio-rad). Bio-beads was first washed extensively with deionized water. After washing, water was decanted from Bio-beads as much as possible using a pipette after centrifugation. Bio-beads was then directly added to the sample in the ratio of 200 mg per 1 ml of the mixed solution. After 45 min of nutation, Bio-beads was removed from the sample by taking out the solution using a pipette after centrifugation at 5000 *g*. The same procedure was repeated three times. We found that this new Bio-beads method improved the yield of protein incorporation into vesicles.

The reconstituted vesicles were concentrated using 100 kDa molecular weight centrifugal filter (Millipore) before taking the EPR spectra. Protein-reconstituted vesicles were characterized with negative-staining electron microscopy. The sample was stained with 1% phosphotungstic acid (pH 6.7) after the protein sample was spread on the 200-mesh formvar and carbon-coated grids. The micrograph (Figure 1B) was taken on a JEOL 1200 EX electron microscope. Most vesicles were ~100 nm in diameter.

All EPR measurements were performed with samples prepared with the Bio-beads method. The EPR binding assay experiments were repeated using samples prepared with the dialysis method for proper comparison with the result from neuronal synaptobrevin. The results from the two methods were identical within experimental uncertainty. Conversely, neuronal SNAREs were reconstituted into vesicles using the Bio-beads method. We observed the complete inhibition of SNARE assembly, identical to our previous results obtained with the samples prepared with the dialysis method (the data are provided as Supplementary data).

EPR data collection and accessibility measurements

EPR spectra were obtained using a Bruker ESP 300 spectrometer equipped with a loop-gap resonator. The accessibility measurements were performed following the procedure described elsewhere (Kweon *et al*, 2002, 2003b).

Fluorescence-quenching experiment

The wild-type sequence of Snc2pF was reconstituted into POPC vesicles containing 15 mol% DOPS, using the dialysis method that was used for the reconstitution of synaptobrevin in our previous work. The concentration of Snc2pF was 5 µM and total lipid concentration was ~2.5 mM. The detailed procedure of the fluorescence experiment is described elsewhere (Kweon *et al*, 2003b). The data were collected at 20°C.

Fusion assays

For lipid-mixing assay, two different vesicle solutions that represent the initial conditions were separately prepared. Chloroform solutions of POPC and DOPS were mixed in a test tube (85:15 mol/mol). Also, 2 mol% each of *N*-(lissamine Rhodamine B sulfonyl)phosphatidylethanolamine (N-Rh-PE) and *N*-(7-nitro-2,1,3-benzoxadiazol-4-yl)phosphatidylethanolamine (N-NBD-PE) were included to a portion of the mixture. After drying the solution with a blow of nitrogen, the test tubes are put in vacuum for several hours for further drying. Snc2pF (or synaptobrevin) was reconstituted into the fraction containing fluorescence labels, while Sso1pHT (or syntaxin) was reconstituted into the unlabeled fraction. The detergent in the samples was removed by the Bio-beads method. The samples were then dialyzed overnight, following the procedure described elsewhere (Kweon *et al*, 2003b), to remove any trace amount of detergent that might interfere with the fluorescence measurements. After dialysis, the solution was centrifuged at

10000g to get rid of protein and lipid aggregates. The lipid-to-protein ratio was aimed at approximately 300:1. Prior to the fusion assay, Sso1pHT-reconstituted vesicles were mixed with Sec9c in a molar ratio of 1:1, and the mixture was incubated at 37°C for 30 min to help the formation of the binary t-SNARE complex. To monitor the lipid mixing, Snc2pF-reconstituted vesicles were mixed with the t-SNARE-reconstituted vesicles in a ratio of 1:9. The final solution contains approximately 1 mM lipids. Fluorescence was measured at excitation and emission wavelengths of 465 and 530 nm, respectively. Fluorescence changes were recorded with a Varian Cary Eclipse model fluorescence spectrophotometer using a quartz cell of 400 µl with the 2 mm path length. We used the same conditions in an attempt to monitor the lipid mixing induced by neuronal SNAREs. We used recombinant Syntaxin 1A without the Habc

domain (SynHT, amino acids 199–288), SNAP-25 (amino acids 1–206), and full-length synaptobrevin (amino acids 1–116) for the fusion assay. Expression, purification, and reconstitution of these neuronal SNAREs are described elsewhere (Kweon *et al*, 2003b).

Supplementary data

Supplementary data are available at *The EMBO Journal* Online.

Acknowledgements

This work was supported by grants from the United States National Institute of Health.

References

- Aalto MK, Ronne H, Keranen S (1993) Yeast syntaxins Sso1p and Sso2p belong to a family of related membrane proteins that function in vesicular transport. *EMBO J* **12**: 4095–4104
- Abrams FS, London E (1992) Calibration of the parallax fluorescence quenching method for determination of membrane penetration depth: refinement and comparison of quenching by spin-labeled and brominated lipids. *Biochemistry* **31**: 5312–5322
- Altenbach C, Greenhalgh DA, Khorana HG, Hubbell WL (1994) A collision gradient method to determine the immersion depth of nitroxides in lipid bilayers: application to spin-labeled mutants of bacteriorhodopsin. *Proc Natl Acad Sci USA* **91**: 1667–1671
- Antonin W, Fasshauer D, Becker S, Jahn R, Schneider TR (2002) Crystal structure of the endosomal SNARE complex reveals common structural principles of all SNAREs. *Nat Struct Biol* **9**: 107–111
- Augustin I, Rosenmund C, Südhof TC, Brose N (1999) Munc13-1 is essential for fusion competence of glutamatergic synaptic vesicles. *Nature* **400**: 457–461
- Brennwald P, Kearns B, Champion K, Keranen S, Bankaitis V, Novick P (1994) Sec9 is a SNAP-25-like component of a yeast SNARE complex that may be the effector of Sec4 function in exocytosis. *Cell* **79**: 245–258
- Brunger AT (2001) Structural insights into the molecular mechanism of calcium-dependent vesicle-membrane fusion. *Curr Opin Struct Biol* **11**: 163–173
- Chapman ER (2002) Synaptotagmin: a Ca²⁺ sensor that triggers exocytosis? *Nat Rev Mol Cell Biol* **3**: 498–508
- Chattopadhyay A, London E (1987) Parallax method for direct measurement of membrane penetration depth utilizing fluorescence quenching by spin-labeled phospholipids. *Biochemistry* **26**: 39–45
- Chen X, Tomchick DR, Kovrigin E, Arac D, Machius M, Südhof TC, Rizo J (2002) Three-dimensional structure of the complexin/SNARE complex. *Neuron* **33**: 397–409
- Chen YA, Scales SJ, Patel SM, Doung YC, Scheller RH (1999) SNARE complex formation is triggered by Ca²⁺ and drives membrane fusion. *Cell* **97**: 165–174
- Couve A, Gerst JE (1994) Yeast Snc proteins complex with Sec9. Functional interactions between putative SNARE proteins. *J Biol Chem* **269**: 23391–23394
- Ferro-Novick S, Jahn R (1994) Vesicle fusion from yeast to man. *Nature* **370**: 191–193
- Gerst JE (2003) SNARE regulators: matchmakers and matchbreakers. *Biochim Biophys Acta* **1641**: 99–110
- Hanson PI, Roth R, Morisaki H, Jahn R, Heuser JE (1997) Structure and conformational changes in NSF and its membrane receptor complexes visualized by quick-freeze/deep-etch electron microscopy. *Cell* **90**: 523–535
- Hu K, Carroll J, Fedorovich S, Rickman C, Sukhodub A, Davletov B (2002) Vesicular restriction of synaptobrevin suggests a role for calcium in membrane fusion. *Nature* **415**: 646–650
- Hubbell ML, Cafiso DS, Altenbach C (2000) Identifying conformational changes with site-directed spin labeling. *Nat Struct Biol* **7**: 735–739
- Hubbell ML, Gross A, Langen R, Lietzow MA (1998) Recent advances in site-directed spin labeling of proteins. *Curr Opin Struct Biol* **8**: 649–656
- Hubbell WL, Mchaourab HS, Altenbach C, Lietzow MA (1996) Watching proteins move using site-directed spin labeling. *Structure* **4**: 779–783
- Jahn R, Lang T, Südhof TC (2003) Membrane fusion. *Cell* **112**: 519–533
- Jahn R, Südhof TC (1999) Membrane fusion and exocytosis. *Annu Rev Biochem* **68**: 863–911
- Katz L, Hanson PI, Heuser JE, Brennwald P (1998) Genetic and morphological analyses reveal a critical interaction between the C-termini of two SNARE proteins and a parallel four helical arrangement for the exocytic SNARE complex. *EMBO J* **17**: 6200–6209
- Kim CS, Kweon DH, Shin YK (2002) Membrane topologies of neuronal SNARE folding intermediates. *Biochemistry* **41**: 10928–10933
- Kweon DH, Kim CS, Shin YK (2002) The membrane-dipped neuronal SNARE complex: a site-directed spin labeling electron paramagnetic resonance study. *Biochemistry* **41**: 9264–9268
- Kweon DH, Kim CS, Shin YK (2003a) Insertion of the membrane-proximal region of the neuronal SNARE coiled coil into the membrane. *J Biol Chem* **278**: 12367–12373
- Kweon DH, Kim CS, Shin YK (2003b) Regulation of neuronal SNARE assembly by the membrane. *Nat Struct Biol* **10**: 440–447
- Lin RC, Scheller RH (1997) Structural organization of the synaptic exocytosis core complex. *Neuron* **19**: 1087–1094
- Lin RC, Scheller RH (2000) Mechanisms of synaptic vesicle exocytosis. *Annu Rev Cell Dev Biol* **16**: 19–49
- Macosko JC, Kim CH, Shin YK (1997) The membrane topology of the fusion peptide region of influenza hemagglutinin determined by spin-labeling EPR. *J Mol Biol* **267**: 1139–1148
- Marash M, Gerst JE (2001) t-SNARE dephosphorylation promotes SNARE assembly and exocytosis in yeast. *EMBO J* **20**: 411–421
- Mchaourab HS, Lietzow MA, Hidek K, Hubbell WL (1996) Motion of spin-labeled side chains in T4 lysozyme. Correlation with protein structure and dynamics. *Biochemistry* **35**: 7692–7704
- McNew JA, Parlati F, Fukuda R, Johnston RJ, Paz K, Paumet F, Sollner TH, Rothman JE (2000) Compartmental specificity of cellular membrane fusion encoded in SNARE proteins. *Nature* **407**: 153–159
- Nicholson KL, Munson M, Miller RB, Filip TJ, Fairman R, Hughson FM (1998) Regulation of SNARE complex assembly by an N-terminal domain of the t-SNARE Sso1p. *Nat Struct Biol* **5**: 793–802
- Pabst S, Margittai M, Vainius D, Langen R, Jahn R, Fasshauer D (2002) Rapid and selective binding to the synaptic SNARE complex suggests a modulatory role of complexins in neuroexocytosis. *J Biol Chem* **277**: 7838–7848
- Parlati F, Weber T, McNew JA, Westermann B, Sollner TH, Rothman JE (1999) Rapid and efficient fusion of phospholipid vesicles by the alpha-helical core of a SNARE complex in the absence of an N-terminal regulatory domain. *Proc Natl Acad Sci USA* **96**: 12565–12570
- Poirier MA, Xiao W, Macosko JC, Chan C, Shin YK, Bennett MK (1998) The synaptic SNARE complex is a parallel four-stranded helical bundle. *Nat Struct Biol* **5**: 765–769
- Protopopov V, Govindan B, Novick P, Gerst JE (1993) Homologs of the synaptobrevin/VAMP family of synaptic vesicle proteins function on the late secretory pathway in *S. cerevisiae*. *Cell* **74**: 855–861

- Rabenstein M, Shin YK (1995) A peptide from the heptad repeat of human immunodeficiency virus gp41 shows both membrane binding and coiled-coil formation. *Biochemistry* **34**: 13390–13397
- Rizo J, Südhof TC (2002) SNAREs and Munc18 in synaptic vesicle fusion. *Nat Rev Neurosci* **3**: 641–653
- Rosenmund C, Sigler A, Augustin I, Reim K, Brose N, Rhee JS (2002) Differential control of vesicle priming and short-term plasticity by Munc13 isoforms. *Neuron* **33**: 411–424
- Rossi G, Salminen A, Rice LM, Brünger AT, Brennwald P (1997) Analysis of a yeast SNARE complex reveals remarkable similarity to the neuronal SNARE complex and a novel function for the C terminus of the SNAP-25 homolog, Sec9. *J Biol Chem* **272**: 16610–16617
- Rothman JE (1994) Mechanisms of intracellular protein transport. *Nature* **372**: 55–63
- Söllner T, Bennett MK, Whiteheart SW, Scheller RH, Rothman JE (1993) A protein assembly-disassembly pathway *in vitro* that may correspond to sequential steps of synaptic vesicle docking, activation, and fusion. *Cell* **75**: 409–418
- Südhof TC (2002) Synaptotagmins: why so many? *J Biol Chem* **277**: 7629–7632
- Sutton RB, Fasshauer D, Jahn R, Brünger AT (1998) Crystal structure of a SNARE complex involved in synaptic exocytosis at 2.4 Å resolution. *Nature* **395**: 347–353
- Thorgeirsson TE, Russell CJ, King DS, Shin YK (1996) Direct determination of the membrane affinities of individual amino acids. *Biochemistry* **35**: 1803–1809
- Weber T, Zemelman BV, McNew JA, Westermann B, Gmachl M, Parlati F, Söllner T, Rothman JE (1998) SNAREpins: minimal machinery for membrane fusion. *Cell* **92**: 759–772
- Weimbs T, Low SH, Chapin SJ, Mostov KE, Bucher P, Hofmann K (1997) A conserved domain is present in different families of vesicular fusion proteins: a new superfamily. *Proc Natl Acad Sci USA* **94**: 3046–3051
- Wimley WC, White SH (1996) Experimentally determined hydrophobicity scale for proteins at membrane interfaces. *Nat Struct Biol* **10**: 842–848
- Yau WM, Wimley WC, Gawrisch K, White SH (1998) The preference of tryptophan for membrane interfaces. *Biochemistry* **37**: 14713–14718